# Surface Functionalization of Magnetite Nanoparticles for Remediation Enhancement of Phenol from Aqueous Solutions

Tanusha Devi Elan Solan,[a,*] Siti Khalijah Mahmad Rozi,[b,c,*] Noorashikin Md Saleh,[a,*] Sharifah Mohamad,[d] Ahmad Razali Ishak,[e] Nurul Yani Rahim,[f] and Monisha Devi Elan Solan [b,*]

Phenol is a toxic pollutant generated by industries. It can diminish the supply of clean water and is hazardous to human health. Hence, an effective abatement method is important to remove phenol from water sources. The following amine-functionalized magnetite nanoparticles, ethylenediamine (EDA), diethylenetriamine (DETA), triethylenetetramine (TETA), tetraethylenepentamine (TEPA), and polyethylenehexamine (PEHA), were used to study the adsorption performances of phenol from the prepared samples. The morphological study revealed long rod shapes with rough and sharp edges, while the elemental analysis presented the addition of two elements, C and N atoms. In addition, the TETA@MNP possessed weaker magnetism compared to MNPs, showing that the surface functionalization of MNPs was successful. TETA@MNP showed the highest percentage for phenol removal compared to others. The TETA@MNP achieved a removal efficiency of 99.2% at optimum conditions of 60 mg dosage, contact time of 25 min, and pH of 7. TETA@MNP obeyed the pseudo-second-order kinetic model and the Freundlich isotherm model, with coefficients of determination ($R^2$) of 0.9765 and 0.9682, respectively. The reusability study has demonstrated that TETA@MNP can be reused approximately 6 times with extremely minor loss. Therefore, TETA@MNP is a good adsorbent for the adsorption of phenol from prepared sample solutions.

*DOI: 10.15376/biores.19.1.456-477*

*Keywords: Amine-functionalized magnetite nanoparticles; Adsorption; Phenol; Water treatment*

*Contact information: a: Department of Chemical and Process Engineering, Faculty of Engineering and Built Environment, Universiti Kebangsaan Malaysia (UKM), 43600 UKM Bangi, Selangor, Malaysia; b: Faculty of Chemical Engineering & Technology, Universiti Malaysia Perlis, Kompleks Pusat Pengajian Jejawi 3, 02600, Arau, Perlis; c: Centre of Excellence for Biomass Utilization, Universiti Malaysia Perlis, Kompleks Pusat Pengajian Jejawi 3, 02600, Arau, Perlis; d: Department of Chemistry, Faculty of Science, University of Malaya, 50603, Kuala Lumpur, Malaysia; e: Centre of Environmental Health and Safety, Faculty of Health Sciences, Universiti Teknologi MARA, Puncak Alam Campus, 42300 Kuala Selangor, Malaysia; f: School of Chemical Sciences, Universiti Sains Malaysia, 11900 Minden, Pulau Pinang, Malaysia; *Corresponding authors:tanushadevi1596@gmail.com: khalijahrozi@unimap.edu.my; noorashikin@ukm.edu.my; monisha97md@gmail.com*

## INTRODUCTION

Water pollution has provoked a global outcry, as it results in the diminishing of water quality. This leads to the scarcity of usable water and expunges food sources, jeopardizing public safety (Abatal *et al.* 2020). Thus, this scenario has violated the second and sixth goals of the United Nations (UN) Sustainability Development Goals (SDGs),

which are zero hunger and access to potable water and sanitation. The main factors for the degradation of water quality are due to rapid population growth, rigorous activities in the agricultural sectors, and intensive industrialization, leading to the fructification of harmful pollutants (Ahamad *et al.* 2019).

Phenol is a volatile aromatic organic compound that exists as a colourless, crystalline solid at room temperature (Al-Trawneh *et al.* 2021). Phenol participates as a significant raw component in the massive production of epoxy resins, synthetic fibre polycarbonate plastics, and phenolic resins (Alves *et al.* 2020; Borah *et al.* 2020). From this, approximately a quarter of the chemicals will be released directly or indirectly into the environment (US EPA 2010). Phenol has a strong tendency to adsorb onto solid matrices, thus proving to be detrimental to aquatic organisms (Erattemparambil *et al.* 2023; Ramin *et al.* 2023). Phenol contributes to the negative impact on the taste and odour of water and fish at relatively low concentrations. The discharge of this chemical is hazardous, as the phenol is corrosive to the skin as well as the mucus membranes (Qu *et al.* 2022). Phenols are considered to be toxic and have adverse effects on the environment. Protein degradation, tissue erosion, central nervous system paralysis, and harm to the human kidney, liver, and pancreas are all caused by drinking phenol-contaminated water for the long term (Al-Trawneh *et al.* 2021; Dehmani *et al.* 2022).

The presence of phenol in the water sources has raised significant environmental concerns among environmentalists. Novel abatement measures are needed to eliminate or neutralize these phenolic compounds from the contaminated water. Adsorption technology is important and ubiquitous in the purification of the water source, as it has been proven to be an efficient and successful method in the removal of the phenolic compounds from polluted water. The adsorption process has proven propitious, as it can be exceptionally efficient, cost-effective, possesses an excellent regenerative capability, can have high selectivity, and is easily installed and maintained. In addition, the adsorption technology offers a good number of flexibilities with different adsorbents, thus allowing for the evaluation of the appropriate adsorbent material with the apical adsorption efficiency as the crucial factor (Jawad *et al.* 2019). Carbon nanotubes, activated carbon, modified diatomite, and mesoporous silica are examples of common adsorbents used for phenol removal. Activated carbon (AC) was the prevalent adsorbent used for the adsorption process during the early stages; however, it has been replaced by the recent developments in new adsorbents of excellent adsorption affinity for various types of pollutants. Ideally, such adsorbents should be ecologically friendly in addition to the adsorbents being able to be recovered and recycled (Kafle 2020; Keshvardoostchokami *et al.* 2021).

Alves *et al.* (2020) mentioned that the integration of the adsorption methods with additional features, such as nanoparticles or magnetism, allows for rapid separation by using electromagnet separated from the water by use of an electromagnet. Such an effect can be turned on and off, which can be advantageous in commercial systems. Thus, by combining the magnetism functionality with the nanoparticles, magnetite nanoparticles (MNPs) are produced and considered critical in industrial pollutant eradication (Baresel *et al.* 2019). The benefits of the MNPs include the improvised effective surface area, minimal toxicity, environmentally friendly nature, maximum biocompatibility, and its recyclability. Despite the advantages, there are a few drawbacks (Begum *et al.* 2021). These include the fact that the bare MNPs are vulnerable to leaching under acidic environments. In addition, direct application can be ineffective, as the particles agglomerate in aqueous media due to van der Waals forces.

The particles also oxidize readily when exposed to the atmosphere. Therefore, employing an appropriate fabrication agent is required to counteract the drawbacks faced by bare MNPs. Chitosan, gelatin, silica, fatty acids, and gold are examples of potential fabrication agents for adsorbents used to overcome the limitations of native MNPs (Gai *et al.* 2020; Naguib *et al.* 2020; Kamaruzaman *et al.* 2023).

Amine compounds are considered excellent choices for the surface fabrication of MNPs, as amines are known for their robust interfacial activity, are chemically stable, and provide wide specific surface areas that allow the adsorption of a significant amount of organic pollutants from the water (Saleh *et al.* 2021). The adsorption capacity of series amine-functionalized magnetite nanoparticles has been significantly improved, thus allowing the adsorption of phenol compounds to be immensely selective, which aids in the rapid removal of these compounds from the aqueous environment. Moreover, the fabrication also provides the adsorption sites for the phenolic compounds via hydrogen bonding and hydrophobic interaction while enhancing the dispersibility and stability of the MNPs (Zhang *et al.* 2019). This statement is supported by the work of Aoopngan *et al.* (2019) with the adsorption of Congo red dyes from water by a novel amine-functionalized magnesium ferrite nanoparticle. This novel adsorbent could be potentially used for phenol removal from water sources. However, there is a lack of studies exploring the series of amines, such as ethylenediamine (EDA), diethylenetriamine (DETA), triethylenetetramine (TETA), tetraethylenepentamine (TEPA), and polyethylenehexamine (PEHA), as the surface-modifying agent to fabricate the surface of MNPs for phenol removal from the aqueous environment. Therefore, it is vital to explore the use of the amine series as the surface fabrication for the MNPs. The formation of the hydrogen bonding, as well as hydrophobic interaction between the series of amine-functionalized magnetite nanoparticles and the phenolic compounds, allows the adsorption of these compounds from the water source (Jawad *et al.* 2019; Ren *et al.* 2023). Moreover, the amine-functionalized magnetite nanoparticles provide adsorption sites for the phenol through hydrogen bonding and hydrophobic interactions (Li *et al.* 2009; Radzali *et al.* 2023). In addition, the amine-functionalized core-shell type MNPs do not generate any secondary pollution during the adsorption and rejuvenation through the leaching. This counteracts the limits of the bare and organically modified MNPs.

Therefore, this research highlights the synthesis of amine-functionalized magnetite nanoparticles, including EDA-functionalized magnetite nanoparticles (EDA@MNP), DETA functionalized magnetite nanoparticles (DETA@MNP), ETA-functionalised magnetite nanoparticles (TETA@MNP), TEPA-functionalized magnetite nanoparticles (TEPA@MNP), and PEHA-functionalized magnetite nanoparticles (PEHA@MNP). Several adsorption parameters, such as contact time, the dosage of adsorbent, initial concentration, and pH of the solution, were studied to obtain an optimum condition for efficient removal of phenol using synthesized adsorbents (You *et al.* 2021). Kinetic and isotherms studies were examined to assess the adsorption mechanism of phenol towards adsorbent (Madzaki *et al.* 2018; Hu *et al.* 2020). The recyclability of the adsorbent was evaluated for six cycles to determine the efficiency and reusability of the adsorbent. The current research highlights the facile synthesis of the amine-functionalized magnetite nanoparticles mainly EDA@MNP, DETA@MNP, TETA@MNP, TEPA@MNP, and PEHA@MNP for the rapid yet effective removal of the phenol from the water.

## EXPERIMENTAL

### Chemicals Used

Iron (II) chloride tetrahydrate ($FeCl_2.4H_2O$) and iron (III) chloride hexahydrate ($FeCl_3.6H_2O$) were purchased from Sigma Aldrich (Burlington, MA, USA) and used as the precursors for the synthesis of magnetite nanoparticles (MNPs). The acetonitrile, hydrochloric acid, sodium hydroxide, analytical grade ethanol (95%), toluene, phenol, and aqueous ammonia were purchased from HmbG Chemical (Darmstadt, Germany). These chemicals were used as received. The EDA, DETA, TETA, TEPA, and PEHA were purchased from Merck (Darmstadt, Germany). The standard stock solution of phenol was prepared at a known concentration of 1000 ppm. The phenol stock solution was prepared by dissolving 0.10 g of phenol in 100 mL of acetonitrile. The phenol stock solution was then stored in the chiller at a temperature of 4 ℃ to prevent degradation. The working standard solutions were prepared freshly by diluting the phenol stock solution with distilled water to the required concentrations.

### Instrumentation

Fourier transform infrared (FTIR) spectroscopy (Perkin Elmer Spectrum-65, Waltham, MA, USA) was used to examine the functional groups present in the adsorbents, primarily EDA@MNP, DETA@MNP, TETA@MNP, TEPA@MNP, and PEHA@MNP. The attenuated total reflectance (ATR) techniques were used in the absorption mode with four scans, at the resolution of ± 4 $cm^{-1}$, with the diamond as the attenuated total reflection (ATR) crystal within the spectral range of 4000 to 400 $cm^{-1}$. The scanning electron microscopy (SEM) images and elemental analysis of the prepared adsorbents were investigated by analytical SEM (JSM-646OLA, JEOL Instruments, Berlin, Germany) equipped with energy-dispersive X-ray (EDX) spectrometry (Carl-Zeiss, Munich, Germany). A vibrating sample magnetometer (MDKFD, Tehran, Iran) was used to characterize the magnetic property (M-H loop) of MNPs and TETA@MNP. The analysis of phenol adsorption in the water was examined using a UV spectrophotometer (Shimadzu, Kyoto, Japan) with a wavelength of 270 nm for phenol. The pH values of the sample solutions were determined using the pH meter (OHAUS Starter 3100, Columbus, OH, USA).

### Preparation of Adsorbent

The preparation of the adsorbent was adapted from the research by Rozi *et al.* (2018). The synthesis of the amine-functionalized magnetite nanoparticles began with the synthesis of the MNPs, which was then followed by the functionalization of amine towards magnetite nanoparticles. At this step, the amine modifying agents used were EDA, DETA, TETA, TEPA, and PEHA (Aoopangan *et al.* 2019).

### Synthesis of the Magnetite Nanoparticles

The MNPs were first produced by the chemical co-precipitation method (Rozi *et al.*2018). According to this method, 6.4 g of $FeCl_2.4H_2O$ and 15.2 g of $FeCl_3.6H_2O$ were measured and dissolved in 320 mL of ultrapure water for the generation of the bare MNPs. The mixture was then stirred rapidly for 2 h at a temperature of 90 ℃. After 2 h, 90 mL of the aqueous ammonia was added directly to the mixture and stirred for another 2 h until a black, conglomerated mixture was formed. The resulting mixture was then cooled to room temperature. For the removal of the unreacted chemicals, the generated nanoparticles were

washed with distilled water and 95% ethanol several times. The resulting product was then sequestered using an external magnet and was oven-dried at 70 °C for 24 h. After the oven-drying process, the generated MNPs were left to cool down at room temperature. They were ground to a fine powder and then stored in a clean, dry container to avoid any contamination. The obtained powder was black in colour and showed high magnetism when in the presence of a magnet (Rozi *et al.* 2018).

## Synthesis of Amine-Functionalized Magnetite Nanoparticles

The amine-functionalized magnetite nanoparticles were synthesized through a one-step co-precipitation method that was adopted by Rozi *et al.* (2018). The freshly prepared MNPs (1.0 g) were dispersed in 10 mL of the amine modifying agent, EDA, which was followed by the addition of 20 mL of toluene. The reaction mixture was stirred vigorously for 2 h at 80 °C and 500 rpm, thus causing the present nanoparticles to be suspended in the solution while allowing the amine to adhere strongly through covalent bonding to the hydroxyl groups that are present on the surface of the MNPs (Ojemaye *et al.* 2017).

After 2 h of stirring, the solution was cooled at room temperature. The resulting black precipitate was then separated using an external magnet. The black precipitate was then washed with a surplus of hot distilled water and 95 % ethanol to remove the unreacted chemicals. The washed black precipitate was then oven-dried for 24 h at a temperature of 70 °C. These procedures were repeated with the other amine modifying agents (DETA, TETA, TEPA, and PEHA). The amine-functionalized magnetite nanoparticles generated were EDA@MNP, DETA@MNP, TETA@MNP, TEPA@MNP, and PEHA@MNP. Figure 1 shows the synthesis of amine-functionalized magnetite nanoparticles.

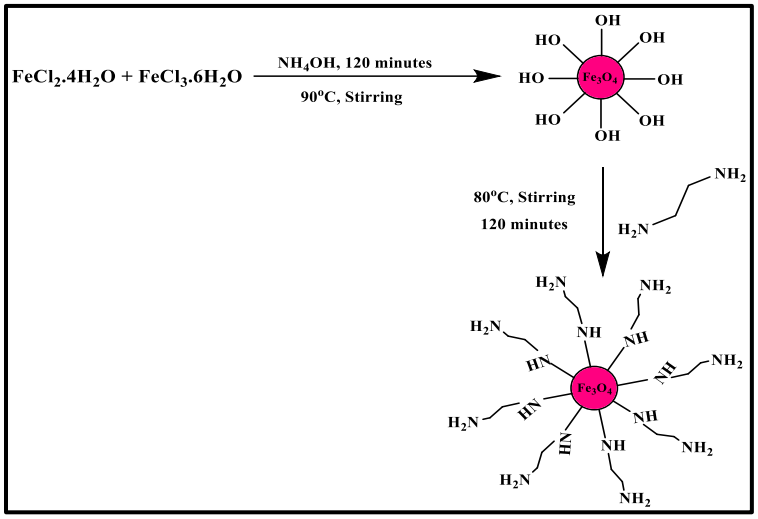


**Fig. 1.** Schematic diagram of the synthesis of amine-functionalized magnetite nanoparticles

## Screening of Optimum Parameters

Several adsorption parameters, such as contact time, the dosage of adsorbent, initial concentration, and pH of the solution, were studied by applying a batch method using 60 mg of selected adsorbent, 10 mL of phenol solution, at a known concentration of 10 ppm, in a tightly sealed vial, and a shaking time of 30 min (250 rpm), at room temperature. The adsorbent was then isolated using an external magnet after the adsorption process before analyzing the analytes with the UV-visible spectrophotometer (UV-Vis) with 10-mm quartz cuvettes (PerkinElmer, Waltham, MA, USA) at the wavelength of 270 nm. The

removal percentage (R%) was calculated using Eq. 1, while the adsorption capacity was calculated using Eq. 2. All the samples were performed in three replicates ($n$ =3) to ensure the accuracy and precision of the results.

*Effect of dosage of adsorbent*

The dosage of adsorbent plays an important factor, as it will affect the efficiency of the adsorption yield. The effects of the dosage of adsorbent on the sorption efficiency were examined towards the phenol. The effect of the dosage of the selected adsorbent on the adsorption process was evaluated by differing the selected adsorbent dosage from 20 to 100 mg with the phenol analyte concentration of 10 ppm at the pH of 7. The required dosage of the selected adsorbent was weighed under a tightly sealed vial and was further evaluated for batch adsorption study.

*Effect of contact time*

The contact time is regarded as an essential parameter for the determination of the competency of the adsorbent. A quick rate of adsorption can be used as an indicator of an effective adsorbent. The effect of contact time on the removal of the phenol using the selected adsorbent was investigated at different time intervals between 5 and 30 min at room temperature to obtain the optimum contact time for adsorption of phenol.

*Effect of initial phenol concentration*

The respective initial amounts of the phenol concentrations greatly affect the removal percentage of these compounds. To determine the relationship between the amount of phenol ions adsorbed on the adsorbent surface and the concentration of the remaining phenol ions in the aqueous phase, the impact of the initial phenol ion concentration on the efficiency of the adsorption process was investigated as a function of the initial concentration. The equilibrium studies were conducted at different initial concentrations of phenol in the range of 5 ppm to 25 ppm at the pH of 7 with the selected adsorbent dosage and contact time.

*Effect of pH of the phenol solution*

The pH of the phenol solution is crucial for the adsorption process because it affects the surface of the adsorbent, binding sites, and the stability of the phenol solution. The adsorption study was completed at various pH values ranging from 3 to 9 at room temperature. The required pH values were adjusted accordingly with the addition of 0.1 M of HCl and 0.1 M NaOH with the aid of a pH meter. The optimum dosage of adsorbent, contact time, and initial concentration values were used for studying this parameter.

*Regeneration and reusability of the selected absorbent*

For the evaluation of the reusability of the selected adsorbent, six cycles of sequential adsorption-desorption cycles were performed. Each of the adsorption processes was performed in batch mode with the optimum parameters using 60 mg as the dosage of adsorbent at a pH of 7 in 10 mL of 10 ppm phenol concentration solution with a contact time of 25 min at 250 rpm at room temperature. After the adsorption process, the phenol-loaded adsorbent was separated from the sample using the external magnet and washed with ethanol first, followed by distilled water several times before entering the next cycle. The effectiveness of the phenol adsorption was determined using Eq. 1:

$$R\,(\%) = \frac{C_I - C_e}{C_i} \times 100 \quad (1)$$

*Adsorption kinetic study*

For this method, the data was examined using the kinetic models of pseudo-first-order and pseudo-second-order. This method was adapted from Younis *et al.* (2020). Lagergren introduced the pseudo-first-order kinetic equation as an adsorption analysis technique, which is shown in Eq. 2,

$$\log\,(q_e - q_t) = \log q_e - \frac{k_1 t}{2.303} \quad (2)$$

where $q_e$ and $q_t$ are the adsorbed (mg) amounts at equilibrium and at time $t$ (min), respectively, and $k_1$ (per min) is the constant adsorption rate.

In contrast, the expression for adsorption kinetics as the pseudo-second-order model is given as Eq. 3,

$$\frac{T}{q_t} = \frac{1}{k_2\, q_e^2} + \frac{1}{q_e}\, t \quad (3)$$

where $k_2$ (g/mg min) is the rate constant determined from the plot slope of $\frac{t}{q_t}$ *versus* $t$.

*Adsorption isotherm study*

The data for the equilibrium adsorption was studied using Langmuir and Freundlich isotherm models. According to Langmuir isotherm, the monolayer adsorption occurs at homogeneous energy level binding sites where there is the absence of interactions between the adsorbed molecules and no transmigration of adsorbed molecules to the adsorption surface occurs. Equation 4 describes the linearised Langmuir isotherm,

$$\frac{1}{q_e} = \frac{1}{k_1 q_m} + \frac{1}{q_m} C_e \quad (4)$$

where the $C_e$ is the solution of phenol at equilibrium concentrate ion ($\frac{mg}{L}$), $q_e$ is the capacity of the adsorption at equilibrium ($\frac{mg}{g}$), $k_1$ is the related constant to the free energy of adsorption ($\frac{L}{mg}$), and $q_m$ is the maximum adsorption capacity at monolayer coverage ($\frac{mg}{g}$). The Freundlich isotherm was applied to predict a heterogeneous adsorbent surface with its adsorption sites at various energy levels (Younis *et al.* 2020). The linear form equation of Freundlich isotherm was expressed as Eq. 5,

$$\ln q_e = \ln K_F + \frac{1}{n} \ln C_e \quad (5)$$

where the Freundlich constant is $K_f$ ($mg^{1-\frac{1}{n}}\, L^{\frac{1}{n}}\, g^{-1}$) and the adsorption capacity and intensity are represented by $n$.

## RESULTS AND DISCUSSION

### Characterisation of Amine-Functionalized Magnetite Nanoparticles

The surface and compositions of the synthesized adsorbents were characterized using FTIR for functional group analysis, SEM for morphological properties analysis, EDX for elemental analysis, and VSM for magnetic property analysis.

Figure 2 shows the presence of the magnetic properties in the bare MNPs displayed an intense characteristic band at ~ 587 $cm^{-1}$. This statement validated the appearance of

the Fe−O peak while the broad O−H stretching band showed its vivid presence at the peak ~ 3425 $cm^{-1}$, thus displaying that the stretching vibration was obtained from the surface hydroxyl groups of bare magnetite nanoparticles (MNPs). The strong peak at ~1451 $cm^{-1}$ was attributed to the physically adsorbed water. The obtained results showed that the bare MNPs had functional groups, such as the hydroxyl groups (OH) and Fe-O groups, which are in agreement with the findings by Boon *et al.* (2019).

Furthermore, in Fig. 2, the spectra of the EDA@MNP displayed three more additional peaks at ~1529 $cm^{-1}$, ~1568 $cm^{-1}$, ~1325 $cm^{-1}$, and ~935 $cm^{-1}$, which were attributed to the N−O bonding, N−$H_2$ scissoring, C−N stretching, and N−H wagging, respectively, thus indicating the layer of EDA on the surface MNPs. In contrast, the bands at ~1332 $cm^{-1}$, ~1542 $cm^{-1}$, ~1572 $cm^{-1}$, and ~1635 $cm^{-1}$ showed C−N stretching, N−O bonding and N−H wagging of −NH− and N−H wagging of the −$NH_2$ distinctly, which demonstrated the presence of DETA in DETA@MNP (Fig. 2) (Aoopngan *et al.* 2019). Moreover, the bands occurring at ~1315 $cm^{-1}$, ~1525 $cm^{-1}$ , ~1569 $cm^{-1}$, and ~1620 $cm^{-1}$ showed the C−N stretching, N−O bonding and N−H wagging of −NH− and N−H wagging of the −$NH_2$ distinctly for the TETA@MNP (Fig. 2), while the bands occurring at ~1329 $cm^{-1}$, ~1511 $cm^{-1}$ ,~1576 $cm^{-1}$, and ~1625 $cm^{-1}$ showed the C−N stretching, N−O bonding and N−H wagging of −NH− and N−H wagging of the −$NH_2$ distinctly for the TEPA@MNP (Fig. 2). In addition, Fig. 2 shows the bands occurring at ~1323 $cm^{-1}$, ~1516 $cm^{-1}$,~1574 $cm^{-1}$, and ~1619 $cm^{-1}$ representing the C−N stretching, N−O bonding and N−H wagging of −NH− and N−H wagging of the −$NH_2$ distinctly for the PEHA@MNP (Li *et al.* 2019; Ojemaye *et al.* 2017).The appearance of these peaks in the FTIR results established that the fabrication of the MNPs with the series of amines groups was successful. Henceforth, these amine modifications generate more active sites for phenol, thus increasing the adsorption efficiency and selectivity of adsorbent towards phenol contaminants.

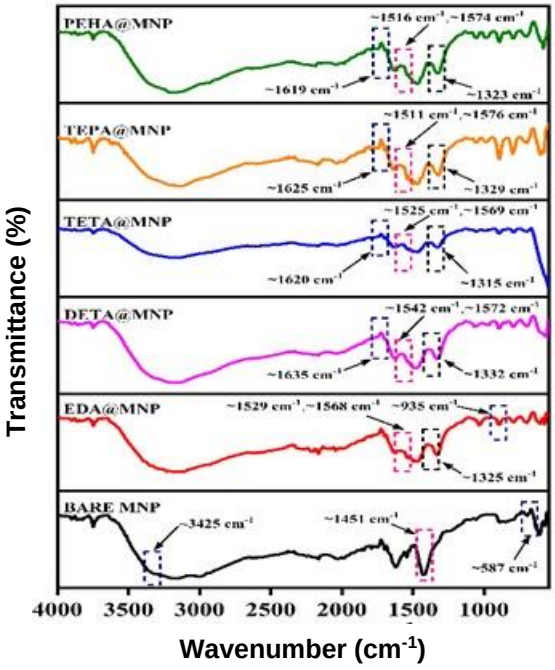


**Fig. 2.** The FTIR spectra of the synthesized adsorbents

The SEM analysis was used to study the morphology of all the nanostructures of the bare MNPs and the series of amine-functionalized magnetite nanoparticles. Based on Fig. 3(A), the bare MNPs displayed a uniform agglomeration size with smooth surface, and the agglomerates were spherical (Li *et al.* 2019). However, after the surface functionalization with the series of amines, the images (Fig. 3(B through F)) showed rough and sharp edges (Dargahi *et al.* 2021).

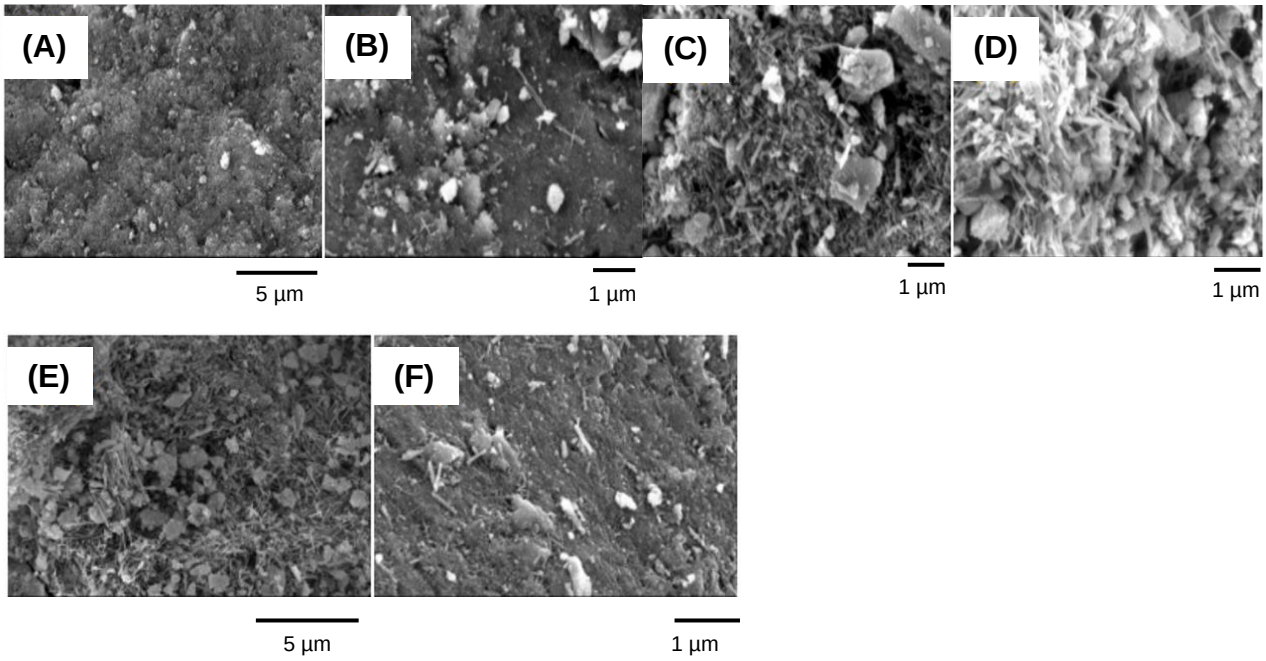


**Fig. 3.** SEM micrographs of (A) bare MNPs, (B) EDA@MNP, (C) DETA@MNP, (D) TETA@MNP, (E) TEPA@MNP, and (F) PEHA@MNP

Elemental analysis was performed to determine the composition of carbon (C), iron (Fe), oxygen (O), and nitrogen (N) for the developed adsorbents. The bare magnetite nanoparticles (MNPs) were composed of only 74.6% of Fe and 25.4% of O, which is shown in Fig. 4(A). This finding agrees with Rozi *et al.* (2018). After the modification of the surface of MNPs, the EDX results presented the addition of two elements, which were the C and N atoms present in the synthesized adsorbents and in agreement with Aoopngan *et al.* (2019).

The composition of the two elements (C and N atoms) increased remarkably from EDA@MNP to PEHA@MNP. EDA@MNP exhibited an additional 23.5% C and 4.1% N (Fig. 4(B)), while DETA@MNP showed an additional 25.9% C and 5.2% N (Fig. 4(C)). In contrast, the TETA@MNP showed an additional 27.7% C and 6.0% N (Fig. 4(D)), while TEPA@MNP displayed an additional 31.2% C and 7.40% N (Fig. 4(E)). PEHA@MNP had the highest compositions of C and N atoms at 34.3% and 9.9%, respectively, as PEHA@MNP possessed the longest amine (alkyl) chain compared to the others. The obtained results demonstrated the successful retention of the series of amines on the surface of magnetite nanoparticles.

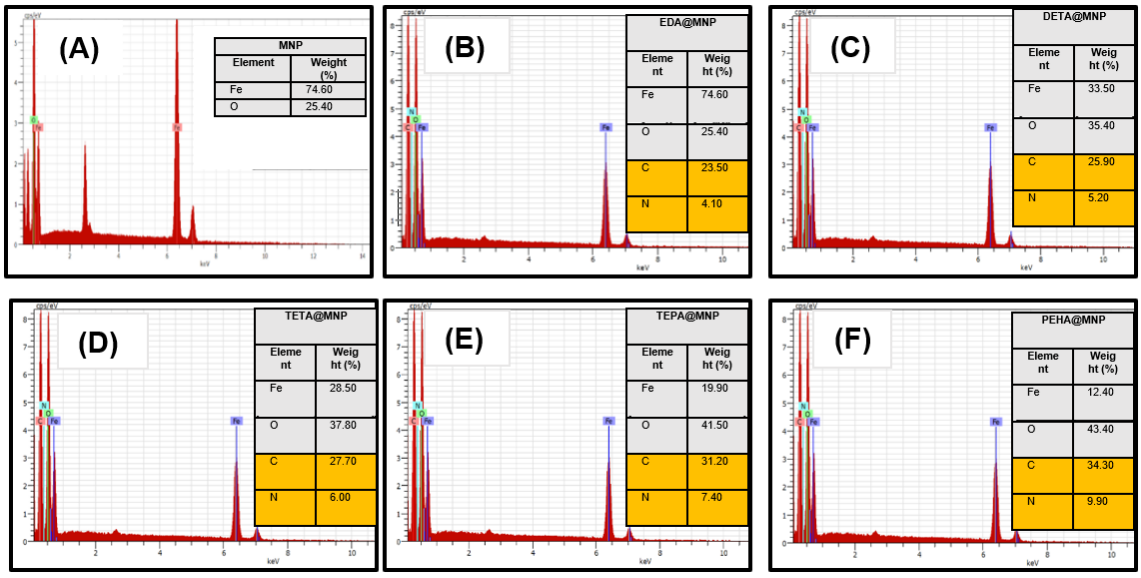


**Fig. 4.** The EDX spectra of (A) bare MNPs, (B) EDA@MNP, (C) DETA@MNP (D) TETA@MNP, (E) TEPA@MNP, and (F) PEHA@MNP

Figure 5 depicts the magnetic hysteresis loops as measured at ambient temperature. MNPs and TETA@MNP were virtually super-paramagnetic, as demonstrated by the M-H curves. The magnetization saturation values of MNPs and TETA@MNP are 93.56 and 75.35 emu $g^{-1}$, respectively. The magnetism of TETA@MNP could be lower due to the interaction of the amine as the surface coating with the magnetic core's surface atoms to create a magnetically disordered layer, hence reducing the total amount of the magnetic phase (Yusoff *et al.* 2018; Ali *et al.* 2021).

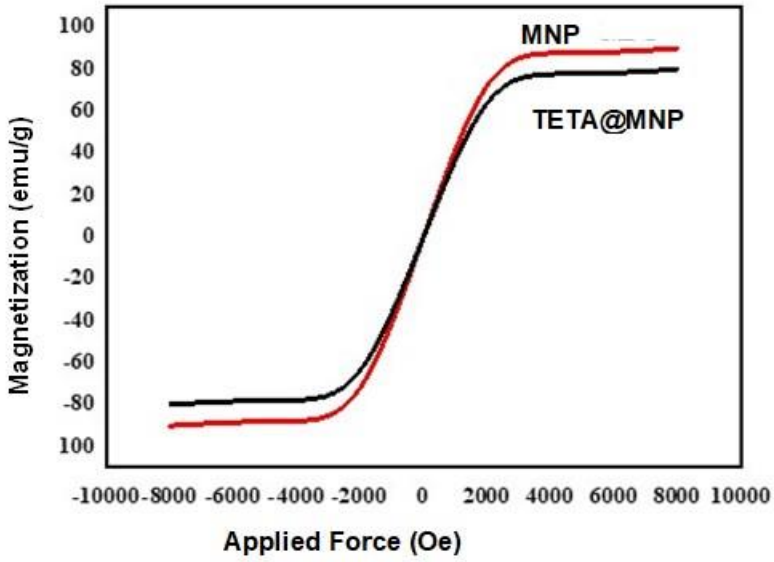


**Fig. 5.** The magnetism of bare MNPs and TETA@MNP

## Application of Amine-Functionalized Magnetite Nanoparticles

After the characterization analyses confirmed the structure and composition of the bare magnetite nanoparticles (MNPs) and the synthesized amine-functionalized magnetite nanoparticles, the prepared adsorbents were then applied in the remediation of phenol from the water.

*Screening of the adsorbents*

The study investigated the adsorption performances of a series of amine-functionalized magnetite nanoparticles, namely EDA@MNP, DETA@MNP, TETA@MNP, TEPA@MNP, and PEHA@MNP, and compared them with bare magnetite nanoparticles (MNPs) for phenol removal. The results showed that the bare MNPs exhibited only modest removal of phenol (44.2%), while the amine-functionalized nanoparticles demonstrated higher removal percentages. Among the series, TETA@MNP displayed the most remarkable performance with a removal percentage of 97.2%.

The researchers attributed TETA@MNP's superior adsorption capabilities to its easy dispersion within the solid support pores, which prevented agglomeration and improved accessibility to active sites. Additionally, TETA's strong interaction with the support hindered amine leaching, ensuring the availability of active sites for adsorption. Its lower steric hindrance compared to other amine-functionalized nanoparticles further enhanced its adsorption performance by reducing mass transfer resistance.

The presence of amine groups on the nanoparticle surfaces provided a considerable advantage, enhancing the interaction system and selectivity of the adsorbents towards phenol. Hydrophobic interactions and hydrogen bonding were identified as the major interaction agents responsible for the increased adsorption capacities of the amine-functionalized magnetite nanoparticles.

Liu *et al.* (2019) supported these findings by explaining that longer amine chains and a higher number of nitrogen atoms provided more active sites for rapid phenol adsorption, leading to higher adsorption capacities.

In contrast, EDA@MNP and DETA@MNP exhibited lower removal percentages due to the saturation of available binding sites, resulting from their shorter amine chains and lower numbers of nitrogen atoms. TEPA@MNP and PEHA@MNP showed reduced removal percentages compared to TETA@MNP due to increased organic steric hindrance, which hindered phenol access to active sites. These findings justify the use of TETA@MNP as the optimum adsorbent for subsequent adsorption studies.

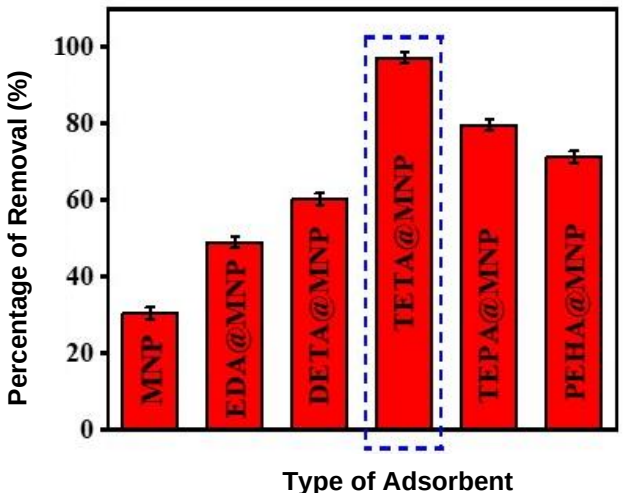


**Fig. 6.** The comparison of the removal (%) of the bare MNPs and the series of amine-functionalized magnetite nanoparticles towards phenol adsorption

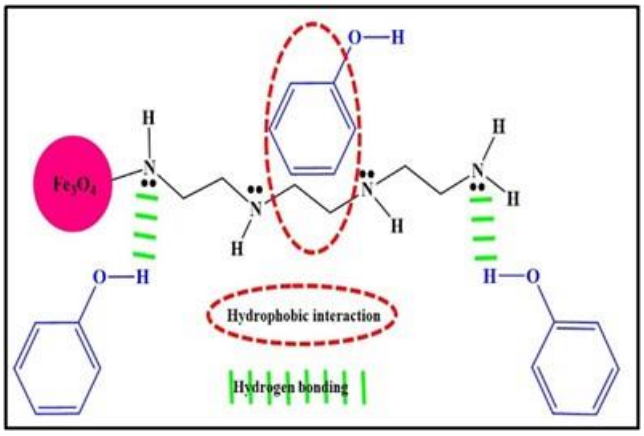


**Fig. 7.** The proposed interaction of TETA@MNP and phenol

## Optimization of Adsorption Studies

For the evaluation of the performance of TETA@MNP as the potential adsorbent for the removal of phenol from the aqueous environment, crucial parameters, such as the dosage of adsorbent (20 mg to 100 mg), contact time (5 min to 30 min), initial phenol concentration (5 ppm to 25 ppm), and pH of phenol solution (3 to 9), were investigated to acquire the optimum conditions to achieve high adsorption efficiencies of phenol.

*Effect of dosage of adsorbent*

The effect of adsorbent dosage on phenol adsorption efficiency was investigated using varying amounts of TETA@MNP adsorbent (20 mg to 100 mg). Figure 8 (A, B) shows that the percentage of phenol removal and adsorption capacity increased rapidly from 20 mg to 60 mg, reaching the highest removal percentage of 98.3% and adsorption capacity of 183 mg/g at 60 mg. This rapid increase can be attributed to the availability of more adsorption sites at higher dosages of adsorbents.

However, beyond 60 mg, the trend showed a slight decrease and remained constant. This was likely due to two main reasons. Firstly, uneven dispersion of the adsorbents resulted in low phenol adsorption capacity. Secondly, the adsorption process reached

equilibrium as the binding sites became saturated with phenol. Additionally, aggregation of adsorbents reduced the surface area exposed and limited the accessibility of active sites for phenol binding, thus causing the levels 80 and 100 mg to be less compatible for this experiment.

These results agreed with a similar study by Zhou *et al.* (2020), where they observed a similar pattern of phenol adsorption capacity using a different type of adsorbent. Based on these findings, the optimum dosage of adsorbent for subsequent phenol adsorption studies was judged to be 60 mg.

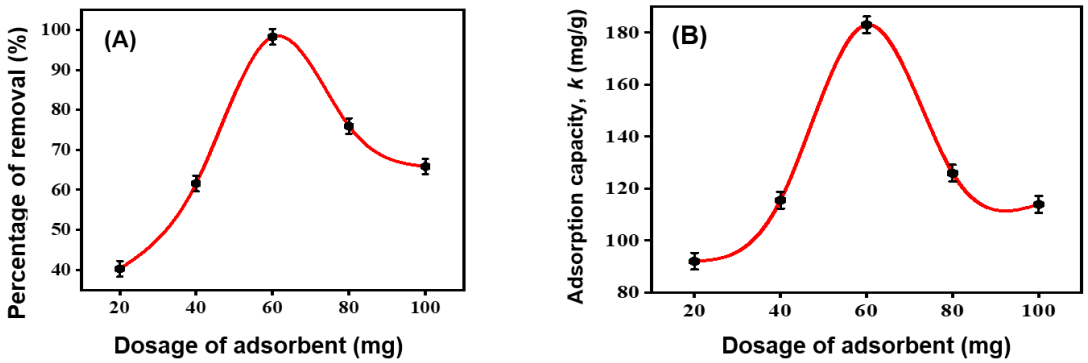


**Fig. 8.** The effect of adsorbent dosage on (A) percentage removal (%) and (B) adsorption capacity (mg/g) of TETA@MNP towards the removal of phenol

*Effect of contact time*

The effect of contact time on phenol adsorption by TETA@MNP was studied at intervals from 5 to 30 min. Figure 9 (A, B) shows the highest removal percentage (94.2%) and adsorption capacity (147 mg/g) at the 25$^{th}$ min. From the 5$^{th}$ to the 25$^{th}$ minute, the percentage of removal and adsorption capacity increased steeply due to abundant vacant active sites on TETA@MNP, allowing effective phenol binding. Prolonging contact time facilitated more collisions, leading to greater adsorption capacity. However, from the 25$^{th}$ to the 30$^{th}$ minute, the trend plateaued, indicating saturation of active binding sites with phenol. The removal percentage (94.3%) and adsorption capacity (145.6 mg/g) at the 30$^{th}$ minute. These findings were consistent with other studies using different adsorbents for phenol removal (Hu *et al.* 2020; You *et al.* 2021). Therefore, 25 min was chosen as the optimum contact time for subsequent phenol adsorption studies using TETA@MNP.

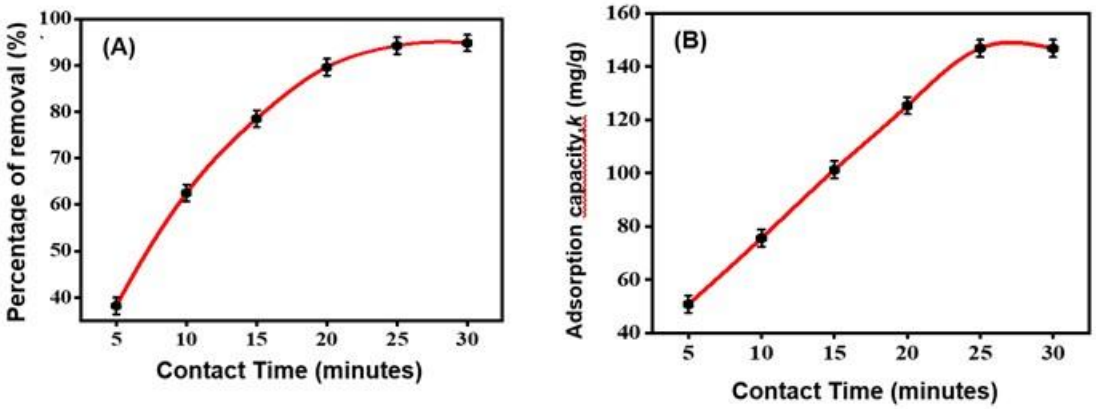


**Fig. 9.** The effect of contact time on (A) percentage removal (%) and (B) adsorption capacity (mg/g) of TETA@MNP towards the removal of phenol

*Effect of initial phenol concentration*

The effect of the initial concentration of phenol solution on its adsorption by TETA@MNP was investigated within the range of 5 to 25 ppm. Figure 10 (A,B) revealed an increasing pattern in the percentage of removal and adsorption capacity of phenol from 5 ppm to 10 ppm. This trend was attributed to the availability of a greater number of active sites on TETA@MNP for phenol binding, resulting in higher adsorption capacity.

The highest percentage of removal (98.6%) and adsorption capacity (164.8 mg/g) were observed at an initial concentration of 10 ppm. However, beyond 10 ppm, the pattern exhibited a decrease. This occurred because the binding sites of TETA@MNP became saturated with phenol, leading to the absence of vacant sites for further binding. Additionally, the high driving force for mass transfer at high initial phenol concentrations caused a drastic decrease in adsorption capacity beyond 10 ppm.

These findings were supported by a similar study using amine-modified activated carbon for phenol adsorption by Saleh *et al.* (2021). Based on the results, the optimum initial concentration of phenol for subsequent adsorption studies was determined to be 10 ppm.

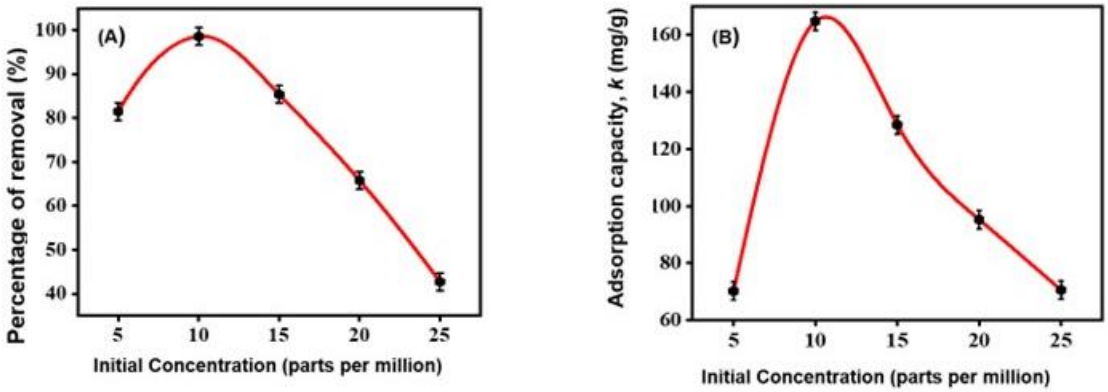


**Fig. 10.** The effect of initial concentration on (A) percentage removal (%) and (B) adsorption capacity (mg/g) of TETA@MNP towards the removal of phenol

*Effect of pH of phenol solution*

The effect of pH on the adsorption of phenol by TETA@MNP was evaluated over a pH range of 3 to 9. Figure 11 (A, B) shows the highest percentage of removal (99.2%) and adsorption capacity (221.5 mg/g) at pH 7. In contrast, lower percentage of removal and adsorption capacity were observed in acidic and basic conditions. This phenomenon was attributed to the presence of available protons ($H^+$) in the solution.

In acidic conditions, the abundance of protons promoted simultaneous protonation of the amine groups on the surface of TETA@MNP and the hydroxyl group of phenol, making both structures cationic. In basic conditions, the lack of available protons induced simultaneous deprotonation of the amine groups on TETA@MNP and the hydroxyl group of phenol, making both structures anionic. In both cases, increased electrostatic repulsion resulted in lower adsorption capacities (Li *et al.* 2019). Many adsorption processes are pH-dependent.

However, at neutral pH, electrostatic repulsion was absent, leading to remarkable adsorption capacity due to increased hydrophobic interactions and hydrogen bonding for effective phenol adsorption by TETA@MNP (Liu *et al.* 2019). In a neutral medium, a wide range of substances can adsorb effectively because their charge or chemical characteristics are less likely to be altered by the pH of the solution. In acidic or basic conditions, the

charge of the adsorbate or the adsorbent may change, making the interaction less favourable. Therefore, pH 7 was judged to be the optimal pH for subsequent phenol adsorption studies using TETA@MNP. It is also suggested that future studies should be conducted for the affinity of the phenolic compounds to the amine-treated magnetite with different pH of solutions should be considered.

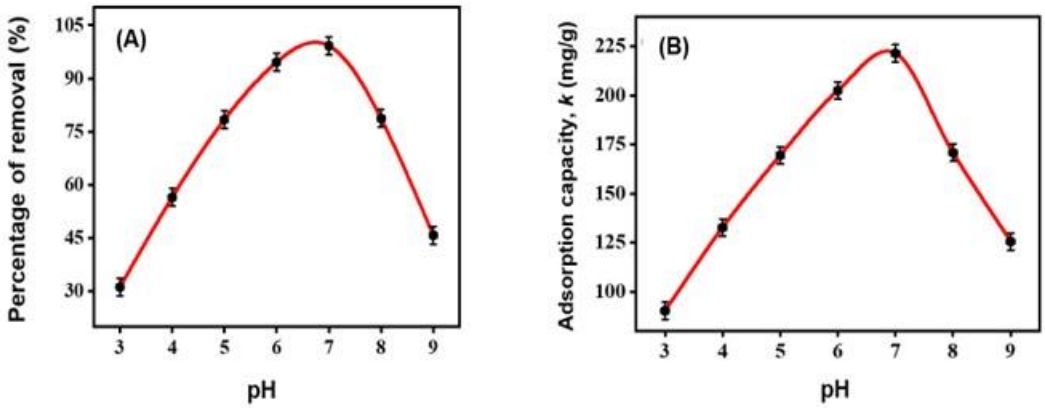


**Fig. 11.** The effect of pH on (A) percentage removal (%) and (B) adsorption capacity (mg/g) of TETA@MNP towards the removal of phenol

*Adsorption kinetic models*

Kinetic studies are crucial in understanding the rate and mechanism of adsorption. In this study, pseudo-first-order and pseudo-second-order kinetic models were explored to study the adsorption of phenol by TETA@MNP. The pseudo-second-order model (Fig. 12 (A-B)) provided the best fit with a coefficient of determination ($R^2$) of 0.9765, compared to 0.8542 for the pseudo-first-order model (Table 1).

**Table 1.** The Kinetic Parameters of the Adsorption of Phenol by TETA@MNP

| Kinetic Models/Constants | Equations/Values |
|---|---|
| **Pseudo-first-order Kinetics** | Ln ($q_e$ - $q_t$) = ln $q_e$- $k_1 t$ |
| $q_e$ (mg $g^{-1}$) | 136.3521 |
| $R_1^2$ | 0.8542 |
| $k_1$ | 0.2737 |
| **Pseudo-second-order Kinetics** | $t/q_t = 1/k^2 q_e^2 + (1/q_e)\ t$ |
| $q_e$ (mg $g^{-1}$) | 221.5125 |
| $R_2^2$ | 0.9765 |
| $k_2$ | 0.0037 |

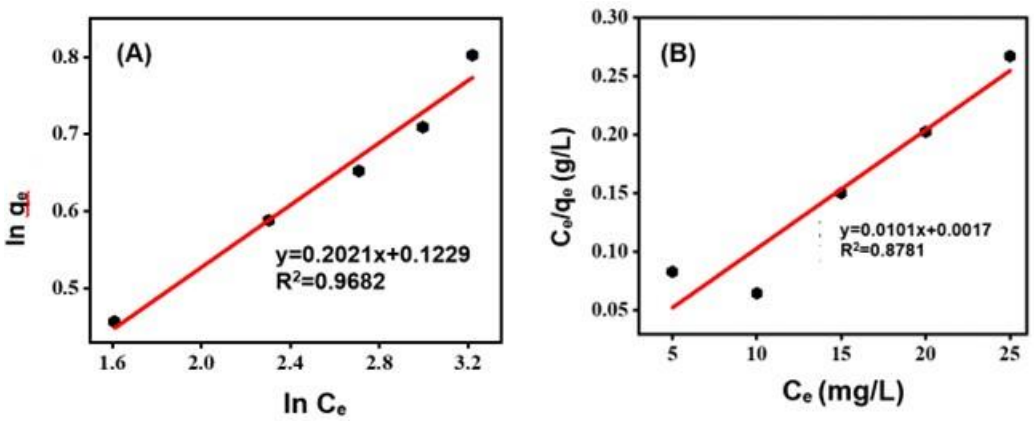


**Fig. 12.** (A)The graph of kinetic model pseudo-first-order plot, (B) graph of kinetic model pseudo-second-order plot

The values in Table 1 indicate that the adsorption process implies that a diffusion mechanism into a porous material had a dominant role in determining the rate (Hubbe *et al.* 2019; Kajjumba *et al.* 2018). A similar study by Wang *et al.* (2022) on phenol adsorption by biochar supports these findings.

*Adsorption isotherm models*

Adsorption isotherm models are essential for understanding the type of adsorption, adsorption capacity, and surface parameters of the adsorbent under equilibrium conditions. In this study, the adsorption of phenol by TETA@MNP was analyzed using the Freundlich and Langmuir isotherm models (Fig. 13 (A-B)). A higher coefficient of determination ($R^2$) for the Freundlich isotherm model (0.9682) relative to the Langmuir isotherm model (0.8781) was observed (Table 2). Thus, the adsorption of phenol by TETA@MNP follows the Freundlich isotherm model, indicating heterogeneous adsorption. The KF and n constants represent the maximum adsorption capacity and intensity, respectively. The obtained KF value of 1.1308 suggests a high tendency of TETA@MNP for phenol adsorption. The "1/*n*" value of 0.2021 indicates a more heterogeneous system, confirming a chemical process rather than a physical process, consistent with the results from the kinetic study (Mishra *et al.* 2022; Al-Ghouti *et al.* 2020; Ariffin *et al*. 2019).

**Table 2.** Isotherm Parameters of the Adsorption of Phenol by TETA@MNP

| Isotherm Models/Constants | Equations/Values |
|---|---|
| **Freundlich Adsorption Isotherm** | $\ln q_e = \ln K_F + 1/n \ln C_e$ |
| $q_e$ (mg $g^{-1}$) | 1.9547 |
| $R_1^2$ | 0.9682 |
| $K_F$ | 1.1308 |
| 1/*n* | 0.2021 |
| **Langmuir Adsorption Isotherm** | $1/q_e = 1/k_1 q_m + (1/q_m) C_e$ |
| $q_e$ (mg $g^{-1}$) | 99.0100 |
| $R_2^2$ | 0.8781 |

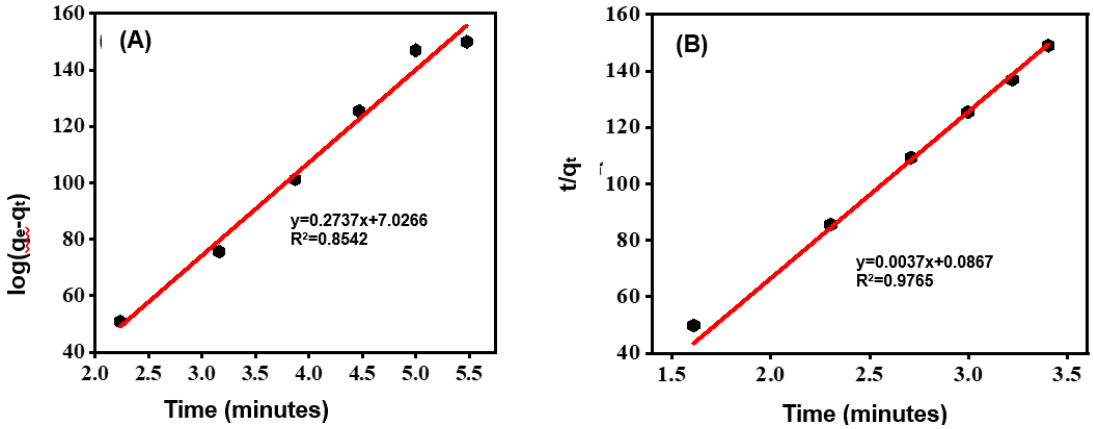


**Fig. 13.** The graphs isotherm models of (A) Freundlich's plot and (B) Langmuir's plot

*Reusability of adsorbent*

It is an important criterion for an exceptional adsorbent to display excellent reusability. Thus, the desorption of the phenol and the regeneration of the TETA@MNP were analyzed in this study. Figure 14 shows that TETA@MNP can be reused approximately 6 times for the adsorption of phenol. As evident from Fig. 14, there was no discernible loss in TETA@MNP recoveries even after six cycles of repetition, hence indicating that TETA@MNP has high stability and reusability efficiency for phenol remediation from aqueous environments. The reusability of TETA@MNP will be able to remarkably cut down the cost of the water treatment in addition to portraying exceptional adsorption capacity. Therefore, TETA@MNP could be suggested as a reliable and potential adsorbent for phenol removal applications, as it can be recycled easily several times.

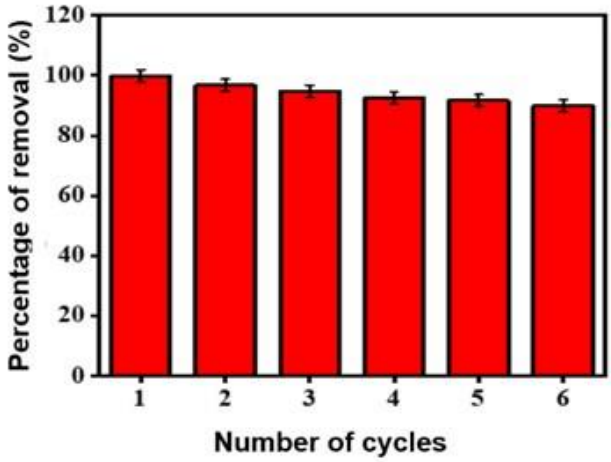


**Fig. 14.** The graph of the reusability of TETA@MNP for adsorption of phenol

*Comparison of amine-functionalized magnetite nanoparticles with other reported adsorbents*

The dosage of adsorbent, contact time, percentage removal, adsorption capacity, kinetic, and isotherm studies of the current adsorbent TETA@MNP were compared with different adsorbents for the adsorption of the phenol from the aqueous environment from previously reported research, which are shown in Table 3.

**Table 3.** Comparison of the Developed Adsorbent with Other Reported Adsorbents

| Adsorbent | Adsorption Capacity (mg/g) | Kinetic Study | Isotherm Study | Percentage Removal (%) | References |
|---|---|---|---|---|---|
| Chitosan eggshell adsorbent | 10.32 | Pseudo-second-order | Langmuir | 65.24 | Xie *et al.* (2020) |
| Iron oxide nanoparticles | 120.60 | Pseudo-second-order | Freundlich | 65.90 | Biehl *et al.* (2018) |
| Acacia glauca saw dust | 34.56 | Pseudo-second-order | Freundlich | - | Dhorabe *et al.* (2019) |
| Biochar | 60.10 | Pseudo-second-order | Langmuir | 86.64 | Liu *et al.* (2019) |
| **TETA@MNP** | **221.50** | **Pseudo-second-order** | **Freundlich** | **99.20** | **This study** |

Based on the results, it is evident that the proposed TETA@MNP is a rapid, reliable, and highly efficient adsorbent with greater adsorption capacity and the highest phenol percentage removal compared to the other reported adsorbents.

## CONCLUSIONS

1. Magnetite nanoparticles that had been modified with triethylenetetramine (TETA@MNP) were found to act as an efficient adsorbent for phenol. Such particles achieved the highest percentage of removal of phenol at 97.2%. The performance was attributed to the ability for magnetic separation, together with a high stability of the suspension in water, as well as rapid adsorption.
2. At optimum conditions, TETA@MNP recorded 99.2% of removal percentage, and the adsorption capacity of 221.5 mg/g which is appropriate for the decontamination of the organic pollutants from the aqueous environment.
3. The adsorption process of the phenol (adsorbate) by TETA@MNP (adsorbent) was found to obey the pseudo-second-order kinetic model and Freundlich isotherm model.
4. A reusability study of TETA@MNP revealed that the synthesized adsorbent was highly recyclable and stable during the phenol adsorption process, as it could be reused at least 6 times without any major loss in the removal efficiency.
5. Therefore, TETA@MNP has been shown to be a sustainable and cost-effective adsorbent for phenol removal applications, as it can selectively adsorb phenol and be recycled several times.

## ACKNOWLEDGEMENT

The authors would like to acknowledge the Fundamental Research Grant Scheme (FRGS), grant number FRGS/1/2022/STG04/UKM/02/7 funded by the Ministry of Higher Education (MOHE) Malaysia and Collaborative Research Grant (9023-00029).

## REFERENCES CITED

Abatal, M., Anastopoulos, I., Giannakoudakis, D. A., and Olguin, M. T. (2020). "Carbonaceous material obtained from bark biomass as adsorbent of phenolic compounds from aqueous solutions," *Journal of Environmental Chemical Engineering* 8(3), article ID 103784. DOI: 10.1016/j.jece.2020.103784

Ahamad, T., Naushad, M., Eldesoky, G. E., Al-Saeedi, S. I., Nafady, A., Al-Kadhi, N. S., Ala'a, H., Khan, A. A., and Khan, A. (2019). "Effective and fast adsorptive removal of toxic cationic dye (MB) from aqueous medium using amino-functionalized magnetic multiwall carbon nanotubes," *Journal of Molecular Liquids* 282, 154-161. DOI: 10.1016/j.molliq.2019.02.128

Al-Ghouti, M. A., and Da'ana, D. A. (2020). "Guidelines for the use and interpretation of adsorption isotherm models: A review," *Journal of Hazardous Materials* 393, article ID 122383. DOI: 10.1016/j.jhazmat.2020.122383

Ali, A., Shah, T., Ullah, R., Zhou, P., Guo, M., Ovais, M., Tan, Z., and Rui, Y. (2021). "Review on recent progress in magnetic nanoparticles: Synthesis, characterization, and diverse applications," *Frontiers in Chemistry* 9, article ID 629054. DOI: 10.3389/fchem.2021.629054

Al-Trawneh, S. A., Jiries, A. G., Alshahateet, S. F., and Sagadevan, S. (2021). "Phenol removal from aqueous solution using synthetic V-shaped organic adsorbent: Kinetics, isotherm, and thermodynamics studies," *Chemical Physics Letters* 781, article ID 138959. DOI: 10.1016/j.cplett.2021.138959

Alves, D. C., Coseglio, B. B., Pinto, L. A., and Cadaval, Jr, T. R. (2020). "Development of Spirulina/chitosan foam adsorbent for phenol adsorption," *Journal of Molecular Liquids* 309, article ID 113256. DOI: 10.1016/j.molliq.2020.113256

Aoopngan, C., Nonkumwong, J., Phumying, S., Promjantuek, W., Maensiri, S., Noisa, P., Pinitsoontorn, S., Ananta, S., and Srisombat, L. (2019). "Amine-functionalized and hydroxyl-functionalized magnesium ferrite nanoparticles for Congo red adsorption," *ACS Applied Nano Materials* 2(8), 5329-5341. DOI: 10.1021/acsanm.9b01305

Ariffin, M. M., Sohaimi, N. M., Yih, B. S., and Saleh, N. M. (2019). "Magnetite nanoparticles coated with surfactant Sylgard 309 and its application as an adsorbent for paraben extraction from pharmaceutical and water samples," *Analytical Methods* 11(32), 4126-4136. DOI: 10.1039/C9AY01147A

Baresel, C., Schaller, V., Jonasson, C., Johansson, C., Bordes, R., Chauhan, V., and Welling, S. (2019). "Functionalized magnetic particles for water treatment," *Heliyon* 5(8), article ID e02325. DOI: 10.1016/j.heliyon.2019.e02325

Begum, S., Yuhana, N. Y., Saleh, N. M., Kamarudin, N. H. N., and Sulong, A. B. (2021). "Review of chitosan composite as a heavy metal adsorbent: Material preparation and properties," *Carbohydrate Polymers* 259, article ID 117613. DOI: 10.1016/j.carbpol.2021.117613

Boon, Y. H., Zain, N. N. M., Mohamad, S., Osman, H., and Raoov, M. (2019). "Magnetic poly (β-cyclodextrin-ionic liquid) nanocomposites for micro-solid phase extraction of selected polycyclic aromatic hydrocarbons in rice samples prior to GC-FID analysis," *Food Chemistry* 278, 322-332. DOI: 10.1016/j.foodchem.2018.10.145

Borah, P., Kumar, M., and Devi, P. (2020). "Types of inorganic pollutants: metals/ metalloids, acids, and organic forms," in: *Inorganic Pollutants in Water*, Elsevier, Amsterdam, Netherlands, pp. 17-31. DOI: 10.1016/B978-0-12-818965-8.00002-0

Dargahi, A., Samarghandi, M. R., Shabanloo, A., Mahmoudi, M. M., and Nasab, H. Z. (2021). "Statistical modeling of phenolic compounds adsorption onto low-cost adsorbent prepared from aloe vera leaves wastes using CCD-RSM optimization: Effect of parameters, isotherm, and kinetic studies," *Biomass Conversion and Biorefinery* 2021, article ID 8404197. DOI: 10.1155/2021/8404197

Dehmani, Y., Dridi, D., Lamhasni, T., Abouarnadasse, S., Chtourou, R., and Lima, E. C. (2022). "Review of phenol adsorption on transition metal oxides and other adsorbents," *Journal of Water Process Engineering* 49, article ID 102965. DOI: 10.1016/j.jwpe.2022.102965

Erattemparambil, K., Mohan, L., Gnanasundaram, N., and Krishnamoorthy, R. (2023). "Insights into adsorption theory of phenol removal using a circulating fluidized bed system," *Arabian Journal of Chemistry* 16(6), article ID 104750. DOI: 10.1016/j.arabjc.2023.104750

Gai, H., Zhang, X., Chen, S., Wang, C., Xiao, M., Huang, T., and Song, H. (2020). "An improved tar–water separation process of low–rank coal conversion wastewater for increasing the tar yield and reducing the oil content in wastewater," *Chemical Engineering Journal* 383, article ID 123229. DOI: 10.1016/j.cej.2019.123229

Hu, L., Guang, C., Liu, Y., Su, Z., Gong, S., Yao, Y., and Wang, Y. (2020). "Adsorption behavior of dyes from an aqueous solution onto composite magnetic lignin adsorbent," *Chemosphere* 246, article ID 125757. DOI: 10.1016/j.chemosphere.2019.125757

Hubbe, M. A., Azizian, S., and Douven, S. (2019). "Implications of apparent pseudo-second-order adsorption kinetics onto cellulosic materials. A review," *BioResources* 14(3), 7582-7626. DOI: 10.15376/biores.14.3.7582-7626

Jawad, A. H., Razuan, R., Appaturi, J. N., and Wilson, L. D. (2019). "Adsorption and mechanism study for methylene blue dye removal with carbonized watermelon (*Citrullus lanatus*) rind prepared *via* one-step liquid phase $H_2SO_4$ activation," *Surfaces and Interfaces* 16, 76-84. DOI: 10.1016/j.surfin.2019.04.012

Kafle, B. P. (2020). "Introduction to nanomaterials and application of UV–visible spectroscopy for their characterization," *Chemical Analysis and Material Characterization by Spectrophotometry* 6, 147-198.

Kajjumba, G. W., Emik, S., Öngen, A., Özcan, H. K., and Aydın, S. (2018). "Modelling of adsorption kinetic processes—errors, theory and application," in: *Advanced Sorption Process Applications*, InTechOpen, London, UK, Available online. DOI: 10.5772/intechopen.80495

Kamaruzaman, N. A., Zin, W. M. K. W. M., Kamarudin, K. H., Saleh, N. M., and Yusoff, F. (2023). "Recent advances in transition metals-based materials as electrocatalysts for water splitting," *International Journal of Electrochemical Science* 18(7), article ID 100187. DOI: 10.1016/j.ijoes.2023.100187

Keshvardoostchokami, M., Majidi, M., Zamani, A., and Liu, B. (2021). "Adsorption of phenol on environmentally friendly $Fe_3O_4$/chitosan/zeolitic imidazolate framework-8

nanocomposite: Optimization by experimental design methodology," *Journal of Molecular Liquids* 323, article ID 115064. DOI: 10.1016/j.molliq.2020.115064

Li, Z., Sellaoui, L., Dotto, G. L., Bonilla-Petriciolet, A., and Lamine, A. B. (2019). "Understanding the adsorption mechanism of phenol and 2-nitrophenol on a biopolymer-based biochar in single and binary systems *via* advanced modeling analysis," *Chemical Engineering Journal* 371, 1-6. DOI: 10.1016/j.cej.2019.04.035

Liu, S., Wang, J., Huang, W., Tan, X., Dong, H., Goodman, B. A., Du, H., Lei, F., and Diao, K. (2019). "Adsorption of phenolic compounds from water by a novel ethylenediamine rosin-based resin: Interaction models and adsorption mechanisms," *Chemosphere* 214, 821-829. DOI: 10.1016/j.chemosphere.2018.09.141

Madzaki, H., Ghani, W. A. W. A. K., Yaw, T. C. S., Rashid, U., and Muda, N. (2018). "Carbon dioxide adsorption on activated carbon hydrothermally treated and impregnated with metal oxides," *Jurnal Kejuruteraan* 30(1), 31-38. DOI: 10.17576/jkukm-2018-30(1)

Mishra, P., Singh, K., and Pandey, G. (2022). "A comparative study of phenol removal by *Pisum-sativum* peels biochars derived at different pyrolysis temperatures: Isotherm, kinetic and thermodynamic modelling," *ChemistrySelect* 7(39), article ID e202202856. DOI: 10.1002/slct.202202856

Naguib, D. M., and Badawy, N. M. (2020). "Phenol removal from wastewater using waste products," *Journal of Environmental Chemical Engineering* 8(1), article ID 103592. DOI: 10.1016/j.jece.2019.103592

Ojemaye, M. O., Okoh, O. O., and Okoh, A. I. (2017). Surface modified magnetic nanoparticles as efficient adsorbents for heavy metal removal from wastewater: Progress and prospects. *Materials Express* 7(6), 439-456.

Qu, Y., Qin, L., Liu, X., and Yang, Y. (2022). "Magnetic $Fe_3O_4$/ZIF-8 composite as an effective and recyclable adsorbent for phenol adsorption from wastewater," *Separation and Purification Technology* 294, article ID 121169. DOI: 10.1016/j.seppur.2022.121169

Radzali, S. A., Markom, M., and Saleh, N. M. (2022). "Parameter effects and optimization in supercritical fluid extraction of phenolic compounds from *Labisia pumila*," *Separations* 9(12), article 385. DOI: 10.3390/separations9120385

Ramin, N. A., Ramachandran, M. R., Saleh, N. M., Mat Ali, Z. M., and Asman, S. (2023). "Magnetic nanoparticles molecularly imprinted polymers: A Review," *Current Nanoscience* 19(3), 372-400. DOI: 10.2174/1573413718666220727111319

Saleh, T. A., Elsharif, A. M., and Bin-Dahman, O. A. (2021). "Synthesis of amine functionalization carbon nanotube-low symmetry porphyrin derivatives conjugates toward dye and metal ions removal," *Journal of Molecular Liquids* 340, article ID 117024. DOI: 10.1016/j.molliq.2021.117024

Wang, P., Tyndall, S., Rahman, T., Roy, P., Jahromi, H., Adhikari, S., and Boersma, M. (2022). "Sorption and recovery of phenolic compounds from aqueous phase of sewage sludge hydrothermal liquefaction using bio-char," *Chemosphere* 287, article ID 131934. DOI: 10.1016/j.chemosphere.2021.131934

Yusoff, M. M., Yahaya, N., Saleh, N. M., and Raoov, M. (2018). "A study on the removal of propyl, butyl, and benzyl parabens *via* newly synthesized ionic liquid loaded magnetically confined polymeric mesoporous adsorbent," *RSC Advances* 8(45), 25617-25635. DOI: 10.1039/C8RA03408G

Zhou, K., Zhang, J., Xiao, Y., Zhao, Z., Zhang, M., Wang, L., and Zhou, C. (2020). "High-efficiency adsorption of and competition between phenol and hydroquinone in aqueous solution on highly cationic amino-poly (vinylamine)-functionalized GO-(o-MWCNTs) magnetic nanohybrids," *Chemical Engineering Journal* 389, article ID 124223. DOI: 10.1016/j.cej.2020.124223

Article submitted: August 4, 2023; Peer review completed: September 30, 2023; Revised version received: October 26, 2023; Revised version approved: October 27, 2023; Published: November 21, 2023.
DOI: 10.15376/biores.19.1.456-477